

## RESEARCH ARTICLE

# Periodic synchronization in a system of coupled phase oscillators with attractive and repulsive interactions

Di Yuan<sup>1,†</sup>, Jun-Long Tian<sup>1,‡</sup>, Fang Lin<sup>1</sup>, Dong-Wei Ma<sup>1</sup>, Jing Zhang<sup>1</sup>, Hai-Tao Cui<sup>1</sup>, Yi Xiao<sup>2</sup>

<sup>1</sup>*School of Physics and Electrical Engineering, Anyang Normal University, Anyang 455000, China*

<sup>2</sup>*School of Physics, Huazhong University of Science and Technology, Wuhan 430074, China*

*Corresponding authors. E-mail: <sup>†</sup>yuandi@aynu.edu.cn; <sup>‡</sup>tjl@aynu.edu.cn*

*Received September 5, 2017; accepted December 28, 2017*

In this study we investigate the collective behavior of the generalized Kuramoto model with an external pinning force in which oscillators with positive and negative coupling strengths are conformists and contrarians, respectively. We focus on a situation in which the natural frequencies of the oscillators follow a uniform probability density. By numerically simulating the model, it is shown that the model supports multistable synchronized states such as a traveling wave state,  $\pi$  state and periodic synchronous state: an oscillating  $\pi$  state. The oscillating  $\pi$  state may be characterized by the phase distribution oscillating in a confined region and the phase difference between conformists and contrarians oscillating around  $\pi$  periodically. In addition, we present the parameter space of the oscillating  $\pi$  state and traveling wave state of the model.

**Keywords** generalized Kuramoto model, pinning force, conformists, contrarians, oscillating  $\pi$  state

**PACS numbers** 05.45.Xt, 89.75.-k

## 1 Introduction

Since its introduction almost 40 years ago, the Kuramoto model of globally coupled oscillators [1] has been established as a paradigmatic model describing Synchronization phenomenon in large populations of coupled oscillators. Similar to the Ising model in the theory of phase transitions [2], the Kuramoto model captures essential features of synchronization observed in many physical systems such as in collective atomic recoil lasers [3, 4], electrochemical oscillators [5, 6], Josephson junction arrays [7, 8], and charge-density waves [10, 11], as well as in a more interdisciplinary context, like for the synchronous flashing of groups of fireflies [12], the rhythm of pacemaker cells of the heart [13], the interaction of cells containing oscillatory chemically reacting constituents [14], phase synchronization in electrical power distribution networks [15–17], and for a large applauding audience [18], for some other systems, see Ref. [19]. Theoretically, the classical Kuramoto model with its generalizations turns out to be the standard for synchronization problem that has inspired a lot of work because of both its simplicity for mathematical treatment and its relevance to practice [2, 19].

In the weak interaction limit, the dynamics of the limit-cycle oscillators could be effectively described in terms of their phase variable  $\phi$  [20]. The original Kuramoto model comprises  $N$  phase oscillators that are globally coupled through the sine of their phase difference. Each oscillator has its own natural frequency  $\omega_i$  chosen from a given probability density  $g(\omega)$  and is characterized by its phase  $\phi_i$ , which is a continuous parametrization of oscillator's evolution with  $2\pi$  gain at completion of each cycle. One of the key assumptions in the Kuramoto model is that the mutual coupling strength  $K$  between an oscillator and the mean field is positive. The oscillators with positive coupling tend to fall in line with neighboring oscillators in favor of the in-phase relationship with them. A natural generalization of it is to allow the coupling strength ( $K$ ) to have either sign. The oscillators with negative coupling drive the oscillators apart to align antiphase with each other. Some authors considered the local interaction among oscillators and found evidence of glassy behavior when both positive and negative coupling strengths were allowed simultaneously [21, 22]. Positive and negative communications coexist in biological systems; some studies have evaluated the significance of these communications on the synchronization in neural networks that

consist of excitatory and inhibitory neurons [23] which interact with their neighboring neurons positively and negatively, respectively. Hong and Strogatz studied the situation in which the coupling strength was regarded as an oscillator's ability to react to the mean field individually [24, 25]. In their work, both positive and negative coupling strengths are present in the population. Conformist oscillators are the ones with positive interaction while contrarian oscillators are those with negative interaction. They found a surprising time-dependent state, a traveling wave state in which the mean field oscillates at a frequency different from the population's mean natural frequency and the phase differences between conformists and contrarians are locked at an angle away from  $\pi$ . Positive and negative interactions are also very common in social systems [26] such as human society. For example, conformists positively interact with the neighbors, following the neighbors' opinion unconditionally, whereas contrarians negatively interact, always rejecting the neighbors' idea.

A natural extension of the generalized Kuramoto model is to add external fields; this gives rise to a much richer dynamical behavior. External fields can model the external current applied to a neuron so as to describe the collective properties of excitable systems with planar symmetry. For other physical devices, such as Josephson junctions, a periodic external force can model an oscillating current across the junctions. The pinning force has been mostly considered in an active rotator model with attractive interaction [27–31]. Shinomoto and Kuramoto studied the phase transition in active rotator systems and found two different regions in the phase diagram: a region of time-periodic physical observables and a region of stable stationary synchronized states [32]. Hong considered a system of coupled phase oscillators under a pinning force and found peculiar dynamic states [33]. However, the effects of pinning force in the system of coupled phase oscillators with attractive and repulsive interactions have not been well explored.

In this study, we have investigated the dynamics and synchronization properties of the generalized Kuramoto model consisting of conformists and contrarians with a pinning force term for fully coupled systems. The effect of pinning force on the collective dynamics in the generalized Kuramoto model coupled via the attractive and repulsive interactions, which is the motivation of this study, has been explored. We have focused on the model with a uniform probability density of natural frequency. In the following, we report our main results.

## 2 Model

The generalized Kuramoto model with both attractive and repulsive interactions under a pinning force consists

of the following set of equations:

$$\dot{\phi}_i = \omega_i + a \sin \phi_i + \frac{K_i}{N} \sum_{j=1}^N \sin(\phi_j - \phi_i), \quad i = 1, 2, \dots, N, \quad (1)$$

where  $\phi_i$ ,  $\omega_i$  and  $K_i$  are the phase, natural frequency, and coupling strength to the mean field, respectively, of the  $i$ th oscillator.  $\omega_i$  is chosen uniform at random from  $[-\gamma, \gamma]$ , here  $\gamma$  is the width of natural frequency distribution.  $K_i$  was chosen randomly from the probability distribution, which for simplicity was assumed to be a double- $\delta$  probability distribution of coupling strengths:  $\Gamma(K) = (1-p)\delta(K - K_-) + p\delta(K - K_+)$ , here  $K_- < 0$  and  $K_+ > 0$  represent the couplings for the contrarians and conformists, respectively, and  $p$  denotes the probability that a random oscillator is a conformist.  $N$  is the number of phase oscillators in the system. The second term on the right-hand side of Eq. (1) is the pinning force introduced to mimic the dynamics of excitable limit-cycle oscillators [32, 33], and  $a$  is the intensity of pinning force. To measure the level of coherence between the oscillators in the model, we employed the mean field-like quantity, namely, the complex order parameter  $Re^{i\Phi}$  which is defined as

$$Z = Re^{i\Phi} = \frac{1}{N} \sum_{j=1}^N e^{i\phi_j}, \quad (2)$$

where the amplitude  $0 \leq R \leq 1$  measures the phase coherence in the population and  $\Phi$  gives the average phase. In terms of  $R$  and  $\Phi$ , Eq. (1) can be rewritten as

$$\dot{\phi}_i = \omega_i + a \sin \phi_i + K_i R \sin(\Phi - \phi_i), \quad i = 1, 2, \dots, N. \quad (3)$$

Eq. (3) expresses the evolution of the  $i$ th oscillator solely in terms of  $R$  and  $\Phi$ . The complex order parameters in conformists and contrarians are also important quantities to determine the dynamics in Eq. (1) and they are defined as  $Z_{\pm} = R_{\pm} e^{i\Phi_{\pm}} = (1/N_{\pm}) \sum_{j \in S_{\pm}} e^{i\phi_j}$ , where  $S_+$  (or  $S_-$ ) means the set of conformists (or contrarians) and  $N_{\pm}$  are the numbers of conformists and contrarians, respectively.  $Z$  is related to  $Z_{\pm}$  by  $Z = \frac{N_-}{N} Z_- + \frac{N_+}{N} Z_+$ .

## 3 Results and analysis

The dynamics given by the Eq. (1) was numerically investigated by a 4th-order Runge–Kutta algorithm at a time step  $\delta t = 0.01$ . The initial sufficient long transient is discarded, after which all quantities of interest were measured. Throughout the work, we let  $N = 10000$ ,

$K_- = -1.0$ ,  $K_+ = 1.5$ ,  $a = 0.01$ , and  $\gamma = 0.05$  unless specified. Initially, the phase of each oscillator was randomly chosen from  $[0, 2\pi]$ .

We started by considering the dynamics of Eq. (1) depending on the fraction of conformists  $p$ . To do this, we investigated the variation of amplitudes of the order parameter  $R$ ,  $R_+$ , and  $R_-$  against  $p$ . The results are presented in Fig. 1. With the increase of  $p$ , the fraction of conformists increases, the system presents several different regimes for different dynamical states as shown in Figure 1. Different dynamics may be distinguished by the phase distributions of oscillators. We investigated the threshold of  $p$  for the different synchronized states. Fig. 1 reveals that synchronized clusters are established once  $p$  becomes nonzero. The blurred  $\pi$  state is stable in the range of  $p < 0.354$ , corresponding to nonuniformly distributed populations of conformists and contrarians on the unit circle. The time evolutions of the phase distributions in Figs. 2(a) and (d) for  $p = 0.2$  show that conformists and contrarians form two partially synchronized clusters, respectively. The peaks of their phase distributions are blurred and are separated from one another by an angle of  $\pi$ . Here, the political interpretation is that two main factions have emerged, in diametric opposition to each other. They could lie anywhere on the political spectrum, but once they emerge, the contrarians oppose the conformists' view. In the range of  $p > 0.596$ ,

the  $\pi$  state is stable in which conformists and contrarians converge to two completely synchronized states. For  $p = 0.9$ , as seen from Figs. 2(c) and (f), the conformists and contrarians form two globally synchronized clusters from the time evolutions of the phase distributions. The phase distributions have one peak each for conformists and contrarians and the two distributions of phases are separated from each other by an angle of  $\pi$ . Figures 2(b) and (e) show that in the range  $0.415 < p < 0.596$ , the

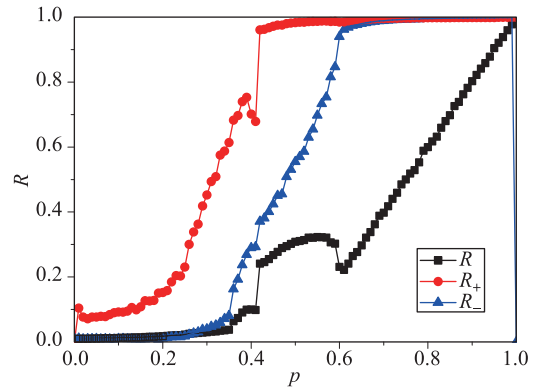


**Fig. 1** Amplitudes of the order parameter  $R$  (square symbol),  $R_-$  (triangle symbol), and  $R_+$  (circle symbol) against the fraction of conformists in the population  $p$ . Here  $K_- = -1.0$ ,  $K_+ = 1.5$ ,  $a = 0.01$ , and  $\gamma = 0.05$ .

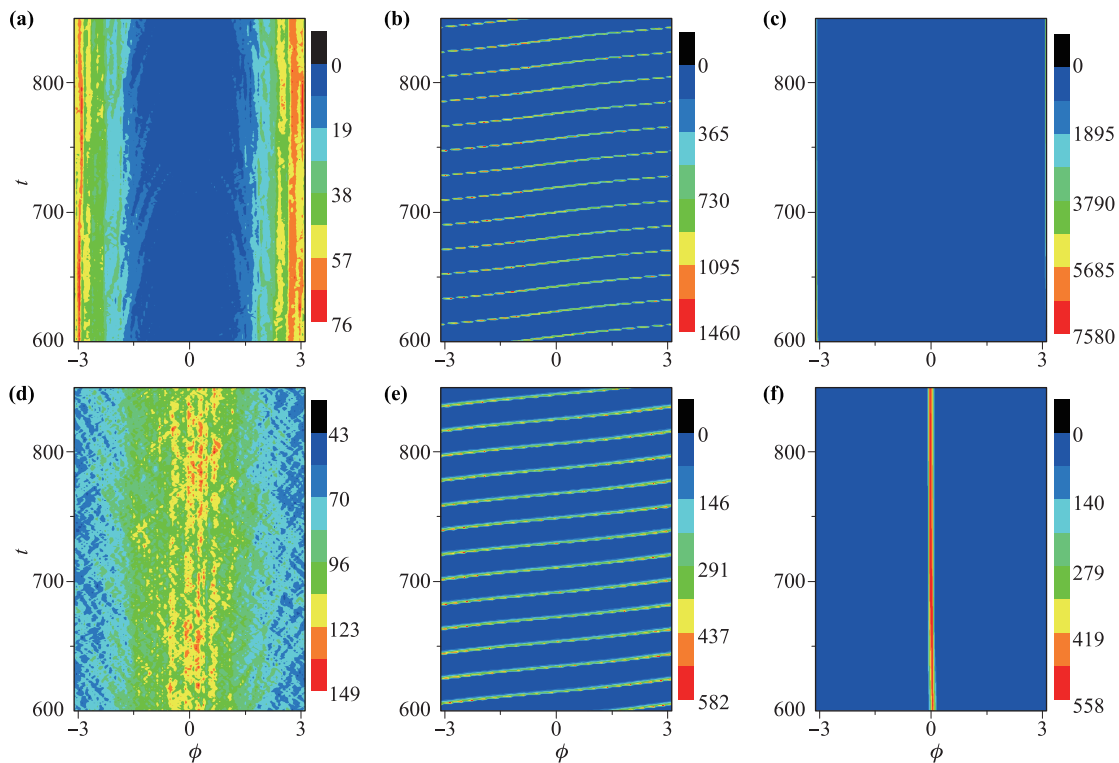


**Fig. 2** Time evolutions of phase distributions in subpopulations of conformists (a–c) and contrarians (d–f). The colors in (a)–(f) represent the number of oscillators, and the specific number can be identified from the color bars. (a, d)  $p = 0.2$ ; (b, e)  $p = 0.5$ ; (c, f)  $p = 0.9$ . Here  $K_- = -1.0$ ,  $K_+ = 1.5$ ,  $a = 0.01$ , and  $\gamma = 0.05$ .

dynamical behavior consists of traveling wave states for  $p = 0.5$ , the phase distributions of contrarians and conformists spontaneously travel along the phase axis always maintaining a separation but not at the angle of  $\pi$ . Here, the conformists are uniform in their views, although the unified view keeps changing, periodically cycling through all possible points of the political spectrum. Meanwhile, the contrarians oppose them, but not completely diametrically, and their opinions remain dispersed throughout.

We have distinguished several dynamical states by means of investigations. However, it is worth pointing out that there still exists another amusing periodic dynamics in Eq. (1). The dynamical states appear during the transition between the blurred  $\pi$  states and traveling wave states. In order to characterize the dynamics, we considered the time evolutions of the phase distributions for the conformists and contrarians which are plotted in Figs. 3(a) and (b), respectively, for  $p = 0.40$ . We all know that the phase distributions of both conformists [ $P_+(\phi)$ ] and contrarians [ $P_-(\phi)$ ] are stationary for the  $\pi$  state while they travel at constant speed  $\Omega$  along the phase axis for a traveling wave state [24]. However, Figs. 3(a) and (b) show an entirely different state:

the phase distributions are neither stationary nor traveling, instead they are oscillating in a confined space with a constant amplitude and period. In order to investigate the periodic dynamics further, we considered how the conformists and contrarians organize themselves in the oscillating states. In order to do it, we arranged all oscillators according to their coupling strengths and natural frequencies. If an oscillator  $i$  has its coupling strength  $K_+$  and an oscillator  $j$  has the coupling strength  $K_-$ , then  $n_i < n_j$  regardless of their natural frequencies, here  $n_i$  and  $n_j$  are the numbers of oscillators  $i$  and  $j$ , respectively;  $n_i < n_j$ , if two oscillators have the same coupling strength but the natural frequencies of oscillators relate as  $\omega_i < \omega_j$ . The time evolution of oscillators' phases is shown in Fig. 3(c). We can clearly see that there exist several synchronous clusters, in which adjacent oscillators stay closely in phase and the phase of each oscillator presents periodic cycling with time. However, Figs. 3(a), (b), and (c) show that the period of phase evolution is same as that of the phase distributions of both conformists and contrarians.

The periodic dynamics of the nonstationary state can also be confirmed according to the evolutions of ampli-

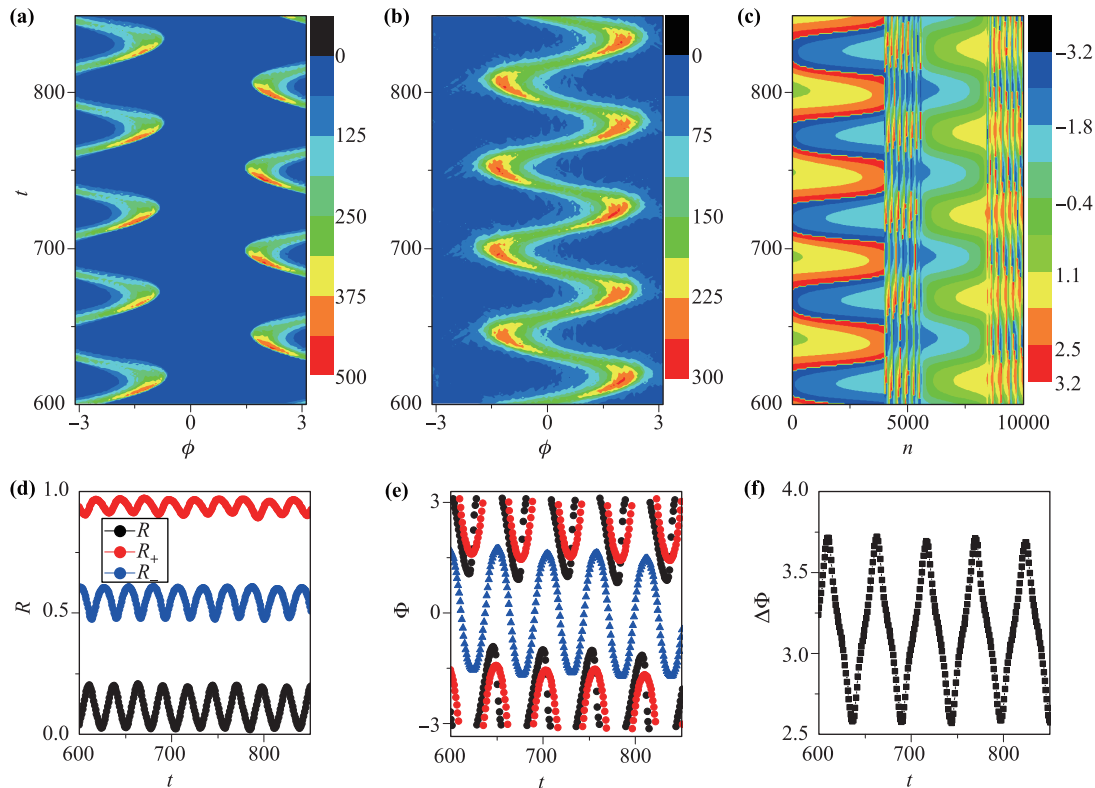


**Fig. 3** Time evolutions of (a, b) phase distributions for subpopulations of conformists and contrarians, respectively. (c) Oscillators' phases, in which the oscillators are ordered according to their coupling strengths and their natural frequencies. Colors in (a)–(c) represent the number of oscillator; specific number can be identified from color bars. (d) Amplitudes  $R$  (black circle symbol),  $R_-$  (blue circle symbol) and  $R_+$  (red circle symbol), of order parameter. (e) Average phases  $\Phi$  (black square symbol),  $\Phi_-$  (blue triangle symbol) and  $\Phi_+$  (red circle symbol). (f) Phase difference  $\Delta\Phi$ .  $\Delta\Phi$  oscillates around  $\pi$  periodically, which refers to an oscillating  $\pi$  state. Here  $K_- = -1.0$ ,  $K_+ = 1.5$ ,  $a = 0.01$ ,  $\gamma = 0.05$ , and  $p = 0.40$ .

tudes,  $R$  and  $R_{\pm}$ , of the order parameter. Figure 3(d) shows the evolutions of amplitudes,  $R$  (black circle symbol),  $R_+$  (red circle symbol) and  $R_-$  (blue circle symbol), of the order parameters. The evolutions of the average phases  $\Phi$  (black square symbol),  $\Phi_+$  (red circle symbol) and  $\Phi_-$  (blue triangle symbol) are shown in Fig. 3(e). It is obvious that three amplitudes of order parameter and the average phases oscillate periodically. Furthermore, Fig. 3(f) presents the evolution of phase difference  $\Delta\Phi$  between contrarians and conformists, which shows that  $\Delta\Phi$  oscillates around  $\pi$  with an amplitude  $A_{\Delta\Phi}$  of about 1.12 rad and with a period of about  $T = 54$  time units and its average over one period stays at  $\pi$ . In this sense, we termed the periodic dynamical state as an oscillating  $\pi$  state.

Before going further, it is necessary to point out that the periodic oscillating  $\pi$  state is different from the oscillating state reported earlier in literature. For instance, Hansel *et al.* [34] found a slow periodic oscillation between two two-cluster states for the case of identical oscillators coupled through the first and the second Fourier modes. Quasiperiodic, periodic and chaotic traveling waves were observed recently in the subset of contrarians, when all the conformists were synchronized, by Burylko *et al.* [35]. Bick *et al.* [36] considered the coupled phase oscillator system with multi-harmonic couplings. The results showed that even symmetric systems of identical oscillators may exhibit chaotic mean field oscillations. In our study, the periodic oscillating  $\pi$  state was found in the model (1). There are three typical characteristics for the oscillating  $\pi$  state. In the first state, the phase distributions of both contrarians and conformists do not travel through the phase space, but they oscillate periodically in a limited region. In the second state, besides the oscillations of amplitudes of the order parameter, the average phases  $\Phi$  and  $\Phi_{\pm}$  are also oscillating periodically, and the phase difference  $\Delta\Phi$  oscillates around  $\pi$  with a constant period and amplitude. In the third state, ad-

acent oscillators stay closely in phase and the phase of each oscillator manifests periodic cycling with time. So, we deem that the periodic oscillating  $\pi$  state found in model (1) could be complementary to the previous work.

It is important to point out that the oscillating  $\pi$  state bifurcates directly from the blurred  $\pi$  state through a continuous transition. The oscillating  $\pi$  state will become unstable when  $p$  is larger than a critical value. Figures 4(a) and (b) show the time evolutions of the average phases  $\Phi$  (the black curve),  $\Phi_+$  (the red curve),  $\Phi_-$  (the blue curve), and the phase difference  $\Delta\Phi$  (the curve in darkcyan) at  $p = 0.414$  and  $p = 0.415$ , respectively. It is obvious that the oscillating  $\pi$  state disappears at  $p = 0.415$  and instead, a traveling wave state shows up: the phase difference  $\Delta\Phi$  does not oscillate around  $\pi$  any more and the average phases  $\Phi$ ,  $\Phi_+$  and  $\Phi_-$  run through the entire range of  $2\pi$ . Together with Fig. 1, Figs. 4(a) and (b) suggest that the oscillating  $\pi$  state yields to a traveling wave state through a discontinuous transition.

To characterize the dependence of the oscillating  $\pi$  state and the traveling wave state on the parameters of  $a$  and  $p$ , two quantities  $\Omega$  and  $\xi$  were introduced.  $\Omega$  is the speed of the traveling wave, and  $\xi$  is the standard deviation of instantaneous wave speed. The speed of the traveling wave is defined as  $\Omega = (1/N) \sum_{j=1}^N \langle \phi_j^g \rangle_t$ , and the standard deviation of instantaneous wave speed is defined as  $\xi = \sqrt{(1/m) \sum_{j=1}^m (\Omega' - \Omega)^2}$ , where  $\Omega'$  is the instantaneous wave speed and  $m$  is the total number of period times. When  $\Omega \neq 0$  and  $\xi = 0$ , the system of coupled phase oscillators displayed a traveling wave behavior. When  $\Omega \neq 0$  and  $\xi \neq 0$ , the system displayed the periodic oscillating  $\pi$  state.  $\Omega$ , the speed of travelling wave, and  $\xi$ , the standard deviation of instantaneous wave speed, are presented as functions of  $a$  and  $p$  in Figs. 5(a) and (b), respectively. Figure 5(a) shows that the traveling wave state occurs in a narrow window. With the increase of  $a$  from zero, the wave speed

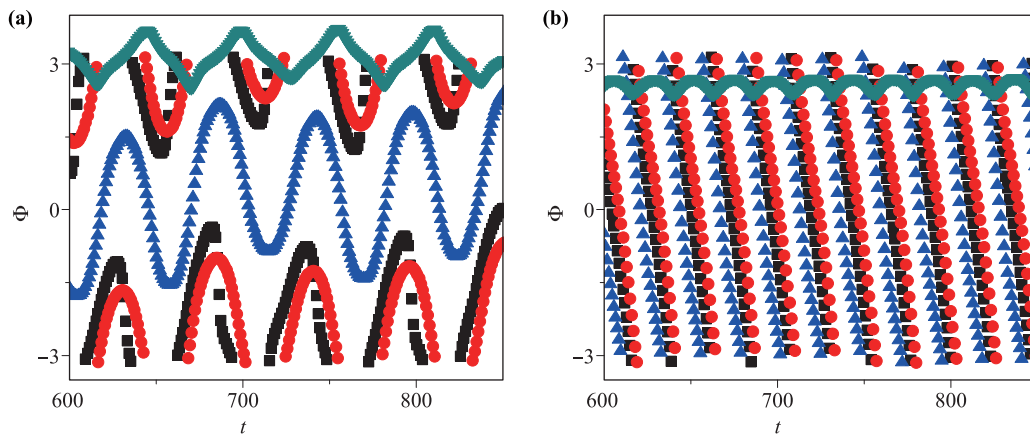


**Fig. 4** (a, b) Evolutions of average phases  $\Phi$  (the curve in black),  $\Phi_+$  (the curve in red),  $\Phi_-$  (the curve in blue) and the phase difference  $\Delta\Phi$  (the curve in darkcyan) for  $p = 0.414$  and  $p = 0.415$ , respectively. Here  $K_- = -1.0$ ,  $K_+ = 1.5$ ,  $a = 0.01$ , and  $\gamma = 0.05$ .

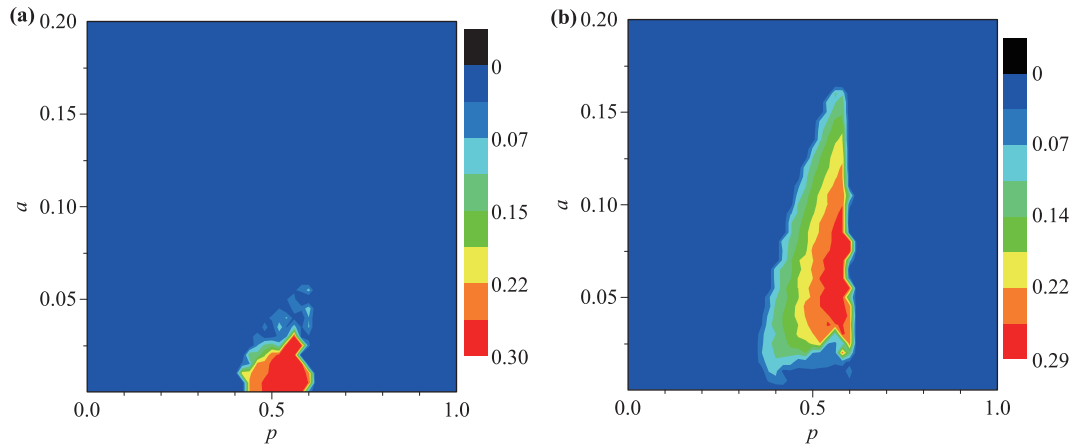


**Fig. 5** The speed of travelling wave ( $\Omega$ ) in (a) and the standard deviation ( $\xi$ ) of instantaneous wave speed in (b) as functions of  $a$  and  $p$ . Here  $K_- = -1.0$ ,  $K_+ = 1.5$ , and  $\gamma = 0.05$ .

decreases gradually. The area in which the  $\pi$  state oscillates increases gradually with increase in the value of  $p$ , as shown in Fig. 5(b). By comparing Figs. 5(a) and (b), we find that the oscillating  $\pi$  state is located at the upper boundary of the travelling wave state. The above results were obtained for  $K_- = -1.0$  and  $K_+ = 1.5$ . For other combinations of  $K_-$  and  $K_+$ , the dependence of the oscillating  $\pi$  state and the traveling wave state on the parameters  $a$  and  $p$  is similar to that in Fig. 5. Note that at the intermediate value of  $p$ , different dynamics of the system can be realized by changing the intensity of pinning force  $a$ , which also reflects the important role of the pinning force on the dynamics of the model (1).

## 4 Conclusions

In this work, we considered the generalized Kuramoto model with an external pinning force in which oscillators with positive coupling strength are conformists, and oscillators with negative coupling strength are contrarians. We focused on a situation in which the natural frequencies of oscillators follow a uniform probability density in the range  $[-\gamma, \gamma]$ . We explored the dynamics of the model in detail and found multistable synchronized states which can be characterized by phase distributions of oscillators. States such as traveling wave states, blurred  $\pi$  state, and  $\pi$  state have already been reported. Specifically, we found an interesting periodic synchronous state that we termed as the oscillating  $\pi$  state. In the oscillating  $\pi$  state, the phase distributions of contrarians and conformists are not stationary but oscillating in a confined region and the phase difference between contrarians and conformists oscillates around  $\pi$  periodically. Furthermore, the oscillating  $\pi$  state may bifurcate from blurred  $\pi$  state at low  $p$  or from a  $\pi$  state

at high  $p$ . We found that when the pinning force is weak enough in comparison with the coupling strength  $K_i$ , the interplay between the pinning force and the mixed interaction of the conformists and contrarians induces a peculiar dynamic state namely, periodic oscillating  $\pi$  state depending on the fraction of the conformists. When the pinning force is absent, the system is found to display three different states: incoherent state, traveling wave state, and  $\pi$  state, depending on the conformist fraction  $p$ . When the weak pinning enters the system, new dynamic states such as the periodic oscillating  $\pi$  state, which are main consequences of the pinning force in the system, appear. When the pinning force is strong enough only the  $\pi$  state (or fully pinned state) is found to exist. We have presented the phase diagram of the model (1) in the parameter space from which the parameter regimes of the oscillating  $\pi$  state and the traveling wave state can be obtained.

**Acknowledgements** The work was supported by the National Natural Science Foundation of China (Grant Nos. 11447001, 11475004, and U1504108), the Key Project of Scientific and Technological Research of the Education Department of Henan Province (Grant Nos. 16A140002, 18A140012, and 18B140001), and the Innovation Foundation for Students of Anyang Normal University (Grant No. ASCX/2017-Z59).

## References

1. Y. Kuramoto, International symposium on mathematical problems in theoretical physics, in: H. Araki (Editor), Lecture Notes in Physics 39 (420–422), New York: Springer 1975
2. S. N. Dorogovtsev, A. V. Goltsev, and J. F. F. Mendes, Critical phenomena in complex networks, *Rev. Mod. Phys.* 80(4), 1275 (2008)

3. C. von Cube, S. Slama, D. Kruse, C. Zimmermann, P. W. Courteille, G. R. M. Robb, N. Piovela, and R. Bonifacio, Self-synchronization and dissipation-induced threshold in collective atomic recoil lasing, *Phys. Rev. Lett.* 93(8), 083601 (2004)
4. J. Javaloyes, M. Perrin, and A. Politi, Collective atomic recoil laser as a synchronization transition, *Phys. Rev. E* 78(1), 011108 (2008)
5. M. Wickramasinghe and I. Z. Kiss, Phase synchronization of three locally coupled chaotic electrochemical oscillators: Enhanced phase diffusion and identification of indirect coupling, *Phys. Rev. E* 83(1), 016210 (2011)
6. I. Z. Kiss, W. Wang, and J. L. Hudson, Populations of coupled electrochemical oscillators, *Chaos* 12(1), 252 (2002)
7. J. W. Swift, S. H. Strogatz, and K. Wiesenfeld, Averaging of globally coupled oscillators, *Physica D* 55(3–4), 239 (1992)
8. K. Wiesenfeld, P. Colet, and S. H. Strogatz, Synchronization transitions in a disordered Josephson series array, *Phys. Rev. Lett.* 76(3), 404 (1996)
9. K. Wiesenfeld, P. Colet, and S. H. Strogatz, Frequency locking in Josephson arrays: Connection with the Kuramoto model, *Phys. Rev. E* 57(2), 1563 (1998)
10. G. Grüner, The dynamics of charge-density waves, *Rev. Mod. Phys.* 60(4), 1129 (1988)
11. C. M. Marcus, S. H. Strogatz, and R. M. Westervelt, Delayed switching in a phase-slip model of charge-density-wave transport, *Phys. Rev. B* 40(8), 5588 (1989)
12. J. Buck and E. Buck, Synchronous fireflies, *Sci. Am.* 234(5), 74 (1976)
13. C. S. Peskin, *Mathematical Aspects of Heart Physiology*, Courant Institute of Mathematical Science Publication, 268–278, New York: Springer, 1975
14. I. Z. Kiss, et al., Emerging coherence in a population of chemical oscillators, *Science* 296(5573), 1676 (2002)
15. G. Filatrella, A. H. Nielsen, and N. F. Pedersen, Analysis of a power grid using a Kuramoto-like model, *Eur. Phys. J. B* 61(4), 485 (2008)
16. M. Rohden, A. Sorge, M. Timme, and D. Witthaut, Self-organized synchronization in decentralized power grids, *Phys. Rev. Lett.* 109(6), 064101 (2012)
17. F. Dorfler, M. Chertkov, and F. Bullo, Synchronization in complex oscillator networks and smart grids, *Proc. Natl. Acad. Sci. USA* 110(6), 2005 (2013)
18. Z. Neda, E. Ravasz, T. Vicsek, Y. Brechet, and A. L. Barabási, Physics of the rhythmic applause, *Phys. Rev. E* 61(6), 6987 (2000)
19. J. A. Acebrón, L. L. Bonilla, C. J. Pérez Vicente, F. Ritort, and R. Spigler, The Kuramoto model: A simple paradigm for synchronization phenomena, *Rev. Mod. Phys.* 77(1), 137 (2005)
20. A. T. Winfree, Biological rhythms and the behavior of populations of coupled oscillators, *J. Theor. Biol.* 16(1), 15 (1967)
21. H. Daido, Population dynamics of randomly interacting self-oscillators, *Prog. Theor. Phys.* 77(3), 622 (1987)
22. C. Börgers, S. Epstein, and N. J. Kopell, Background gamma rhythmicity and attention in cortical local circuits: A computational study, *Proc. Natl. Acad. Sci. USA* 102(19), 7002 (2005)
23. C. Börgers and N. Kopell, Synchronization in networks of excitatory and inhibitory neurons with sparse, random connectivity, *Neural Comput.* 15(3), 509 (2003)
24. H. Hong and S. H. Strogatz, Kuramoto model of coupled oscillators with positive and negative coupling parameters: An example of conformist and contrarian oscillators, *Phys. Rev. Lett.* 106(5), 054102 (2011)
25. H. Hong and S. H. Strogatz, Conformists and contrarians in a Kuramoto model with identical natural frequencies, *Phys. Rev. E* 84(4), 046202 (2011)
26. C. Freitas, E. Macau, and A. Pikovsky, Partial synchronization in networks of non-linearly coupled oscillators: The Deserter Hubs Model, *Chaos* 25(4), 043119 (2015)
27. H. Sakaguchi, Cooperative phenomena in coupled oscillator systems under external fields, *Prog. Theor. Phys.* 79(1), 39 (1988)
28. H. Kori and A. S. Mikhailov, Strong effects of network architecture in the entrainment of coupled oscillator systems, *Phys. Rev. E* 74(6), 066115 (2006)
29. T. M. Jr Antonsen, R. T. Faghih, M. Girvan, E. Ott, and J. Platig, External periodic driving of large systems of globally coupled phase oscillators, *Chaos* 18(3), 037112 (2008)
30. E. Ott and T. M. Antonsen, Low dimensional behavior of large systems of globally coupled oscillators, *Chaos* 18(3), 037113 (2008)
31. S. H. Park and S. Kim, Noise-induced phase transitions in globally coupled active rotators, *Phys. Rev. E* 53(4), 3425 (1996)
32. S. Shinomoto and Y. Kuramoto, Phase transitions in active rotator systems, *Prog. Theor. Phys.* 75(5), 1105 (1986)
33. H. Hong, Periodic synchronization and chimera in conformist and contrarian oscillators, *Phys. Rev. E* 89(6), 062924 (2014)
34. D. Hansel, G. Mato, and C. Meunier, Clustering and slow switching in globally coupled phase oscillators, *Phys. Rev. E* 48(5), 3470 (1993)
35. O. Burylko, Y. Kazanovich, and R. Borisjuk, Bifurcation study of phase oscillator systems with attractive and repulsive interaction, *Phys. Rev. E* 90(2), 022911 (2014)
36. C. Bick, M. Timme, D. Paulikat, D. Rathlev, and P. Ashwin, Chaos in symmetric phase oscillator networks, *Phys. Rev. Lett.* 107(24), 244101 (2011)